



Universiteit  
Leiden  
The Netherlands

## **Absence of functional autoantibodies targeting angiotensin II Receptor type 1 and endothelin-1 type A receptor in circulation and purified IgG from patients with systemic sclerosis**

Oostveen, W.M. van; Hoekstra, E.M.; Levarht, E.W.N.; Kotliar, I.B.; Sakmar, T.P.; Toes, R.E.M.; ... ; Fehres, C.M.

### **Citation**

Oostveen, W. M. van, Hoekstra, E. M., Levarht, E. W. N., Kotliar, I. B., Sakmar, T. P., Toes, R. E. M., ... Fehres, C. M. (2024). Absence of functional autoantibodies targeting angiotensin II Receptor type 1 and endothelin-1 type A receptor in circulation and purified IgG from patients with systemic sclerosis. *Arthritis & Rheumatology*, 77(7), 901-913. doi:10.1002/art.43099




Version: Publisher's Version

License: [Creative Commons CC BY-NC-ND 4.0 license](https://creativecommons.org/licenses/by-nc-nd/4.0/)

Downloaded from: <https://hdl.handle.net/1887/4212129>

**Note:** To cite this publication please use the final published version (if applicable).

# Absence of Functional Autoantibodies Targeting Angiotensin II Receptor Type 1 and Endothelin-1 Type A Receptor in Circulation and Purified IgG From Patients With Systemic Sclerosis

Wieke M. van Oostveen,<sup>1</sup>  Eva M. Hoekstra,<sup>1</sup>  E. W. Nivine Levarht,<sup>1</sup> Ilana B. Kotliar,<sup>2</sup> Thomas P. Sakmar,<sup>3</sup> René E. M. Toes,<sup>1</sup> Jeska K. de Vries-Bouwstra,<sup>1</sup> Laura H. Heitman,<sup>4</sup> and Cynthia M. Fehres<sup>1</sup> 

**Objective.** Systemic sclerosis (SSc) is a rare but severe autoimmune disease characterized by immune dysregulation, fibrosis, and vasculopathy. Although previous studies have highlighted the presence of functional autoantibodies targeting the angiotensin II receptor type 1 (AT<sub>1</sub>) and endothelin-1 type A receptor (ET<sub>A</sub>R), leading to autoantibody-mediated receptor stimulation and subsequent activation of endothelial cells (ECs), a comprehensive understanding of the direct interaction between these autoantibodies and their receptors is currently lacking. Moreover, existing data confirming the presence of these autoantibodies in SSc often rely on similar methodologies and assays. Our aim was to replicate previous findings and to investigate the functional effects of IgG derived from patients with SSc (SSc IgG) on AT<sub>1</sub> and ET<sub>A</sub>R signaling, the downstream EC response, and the presence of AT<sub>1</sub>-binding autoantibodies in circulation.

**Methods.** Quantitative polymerase chain reaction and cytokine enzyme-linked immunosorbent assay, alongside a real-time cell analyzer, were used to assess receptor-specific functional characteristics of purified SSc IgG (n = 18). Additionally, a novel protein capture assay using solubilized epitope-tagged AT<sub>1</sub> was developed to detect AT<sub>1</sub>-binding autoantibodies in plasma samples from patients with SSc (n = 28) and healthy donors (n = 14).

**Results.** No evidence for EC activation in an AT<sub>1</sub>- or ET<sub>A</sub>R-dependent manner was revealed. Furthermore, stimulation with SSc IgG did not induce receptor activation or alter G protein-coupled receptor signaling on agonist stimulation in a model with receptor overexpression. Lastly, no AT<sub>1</sub>-binding autoantibodies were detected in plasma samples from patients with SSc when using epitope-tagged solubilized AT<sub>1</sub>.

**Conclusion.** Overall, our study did not provide evidence to support the presence of AT<sub>1</sub>- or ET<sub>A</sub>R-activating autoantibodies in purified SSc IgG or AT<sub>1</sub>-binding autoantibodies in the circulation of patients with SSc.

## INTRODUCTION

Systemic sclerosis (SSc) is a rheumatic autoimmune disorder characterized by microangiopathy, including Raynaud phenomenon (RP), immune dysregulation, and fibrosis of the skin and internal organs.<sup>1</sup> Clinical presentation of SSc vary from an indolent form with limited deterioration to rapidly progressive disease, associated with irreversible organ damage and relatively high mortality rates.<sup>2</sup> Despite its rarity, SSc poses a significant clinical

challenge because of its clinical heterogeneity and potential for a high mortality rate.<sup>3</sup> More than 95% of patients with SSc test positive for antinuclear antibodies (ANAs) including anti-topoisomerase I antibodies (ATA) and anticentromere antibodies (ACA). The presence of ATA and ACA is disease specific. The two antibodies rarely co-occur and are associated with distinct clinical phenotypes.<sup>4</sup> Although the underlying pathologic mechanisms in SSc subtypes remain largely elusive, the presence of ANA and RP precedes clinical disease and fibrosis onset, indicating a potential link between

<sup>1</sup>Wieke M. van Oostveen, MSc, Eva M. Hoekstra, MD, MSc, E. W. Nivine Levarht, BSc, René E. M. Toes, PhD, Jeska K. de Vries-Bouwstra, MD, PhD, Cynthia M. Fehres, PhD: Leiden University Medical Center, Leiden, The Netherlands; <sup>2</sup>Ilana B. Kotliar, PhD: The Rockefeller University and Tri-Institutional PhD Program in Chemical Biology, New York, New York; <sup>3</sup>Thomas P. Sakmar, MD: The Rockefeller University, New York, New York; <sup>4</sup>Laura H. Heitman, PhD: Leiden University and Oncode Institute, Leiden, The Netherlands.

Additional supplementary information cited in this article can be found online in the Supporting Information section (<http://onlinelibrary.wiley.com/doi/10.1002/art.43099>).

Author disclosures are available at <https://onlinelibrary.wiley.com/doi/10.1002/art.43099>.

Address correspondence via email to Cynthia M. Fehres, PhD, at [c.m.fehres@lumc.nl](mailto:c.m.fehres@lumc.nl).

Submitted for publication September 12, 2024; accepted in revised form December 11, 2024.

autoimmunity and vasculopathy. A deeper understanding of disease pathogenesis could facilitate early intervention to halt fibrosis and disease progression.

RP, an early but nonspecific sign of SSc, is characterized by restricted blood flow to the extremities due to endothelial cell (EC) dysregulation and exaggerated vasoconstriction.<sup>5</sup> This vasoconstrictive response, along with vasodilation, is regulated by the renin-angiotensin-system, with angiotensin II (AngII) and its receptor angiotensin II type 1 (AT<sub>1</sub>) playing pivotal roles.<sup>6,7</sup> Additionally, endothelin-1 (ET-1), a proinflammatory peptide, contributes to vasoconstriction by activating endothelin-1 type A receptor (ET<sub>A</sub>R), implying potential involvement for AngII and ET-1 in SSc pathogenesis.<sup>8</sup> Indeed, the use of angiotensin-converting enzyme inhibitors in SSc has been associated with reduced death from renal crisis, although no effect on RP was found.<sup>9,10</sup> Furthermore, several clinical trials have investigated the effects of AT<sub>1</sub> and ET<sub>A</sub>R inhibitors to reduce disease manifestations, such as fibrosis, pulmonary arterial hypertension, and digital ulcers. Although these blockers alleviated vascular complications, no effect on fibrosis in skin or other organs was observed, thereby highlighting the need for further research into the role of AT<sub>1</sub> and ET<sub>A</sub>R in SSc pathophysiology.<sup>11–15</sup>

Previous studies have reported the presence of autoantibodies against AT<sub>1</sub> and ET<sub>A</sub>R in SSc,<sup>16–19</sup> as well as in other diseases, including preeclampsia and renal-allograft rejection.<sup>20–22</sup> In SSc, high autoantibody levels predicted disease-related death and thus were proposed as biomarkers for risk assessment for disease progression.<sup>19</sup> These autoantibodies are defined to act as agonists, as they activate the receptor and its downstream signaling cascade.<sup>20–23</sup> Both AT<sub>1</sub> and ET<sub>A</sub>R are members of the G protein-coupled receptor (GPCR) family, which are membrane-bound proteins characterized by seven transmembrane helices and intracellular coupling to heterotrimeric G proteins composed of  $\alpha$ ,  $\beta$ , and  $\gamma$  subunits.<sup>24</sup> On agonist ligand stimulation, GPCRs activate various downstream signaling pathways through coupling to G proteins or via  $\beta$ -arrestins.<sup>25</sup> Activated AT<sub>1</sub> and ET<sub>A</sub>R primarily couple to G $\alpha_{q/11}$  leading to increased cytosolic Ca<sup>2+</sup> and subsequent vasoconstriction.<sup>26–28</sup>

The contribution of AT<sub>1</sub> and ET<sub>A</sub>R activation to vasoconstriction and the reported presence of autoantibodies targeting AT<sub>1</sub> and ET<sub>A</sub>R in SSc suggest a potential contribution of agonistic anti-AT<sub>1</sub>- and anti-ET<sub>A</sub>R autoantibodies to vasculopathy in SSc. However, detailed studies examining the direct interaction between these autoantibodies and their receptors are currently lacking.<sup>18,28</sup> Therefore, the present study aimed to investigate the functional effects of IgG derived from patients with SSc (SSc IgG) on AT<sub>1</sub> and ET<sub>A</sub>R signaling, as well as its downstream EC response. To this end, in addition to conventional techniques such as quantitative polymerase chain reaction (qPCR) and cytokine enzyme-linked immunosorbent assay (ELISA), a real-time cell analyzer (RTCA), well-validated for studying GPCR pharmacology, was used to assess functional characteristics of SSc IgG in

a direct and receptor-specific manner. Additionally, a novel protein capture assay using solubilized receptors was established to evaluate the presence of anti-AT<sub>1</sub> autoantibodies in the circulation of patients with SSc.

## MATERIALS AND METHODS

**Patients and healthy individuals.** Plasma and serum samples were collected from patients with SSc who were part of a prospective cohort study (the Leiden Combined Care in Systemic Sclerosis cohort) at the Leiden University Medical Center's Rheumatology outpatient clinic. Patient characteristics are detailed in Supplementary Table 1. Patients with both low and high levels of anti-AT<sub>1</sub> (cutoff = 9.5) and anti-ET<sub>A</sub>R antibodies (cutoff = 10.4) were included, as measured in serum by Riemekasten et al,<sup>19</sup> as previously reported. All patients met the American College of Rheumatology/EULAR 2013 criteria for the classification of SSc and had not undergone hematopoietic stem cell transplantation.<sup>29</sup> The study was approved by the Leiden University Medical Center ethical review board (protocol P17.151). Written informed consent was obtained from both patients and healthy donors (HDs).

**Purification of IgG antibodies.** IgG antibodies were purified from plasma using a 1-mL HiTrap Protein G HP affinity column (GE29-0485-81; Cytiva), followed by a direct buffer exchange using a 53-mL HiPrep 26/10 desalting column (GE17-5087-01; Cytiva). Isolated IgG was concentrated to 4 to 26 mg/mL using Amicon Ultra-15 50 kDa filter devices (UFC9050; Merck) and potential endotoxins were removed with Pierce High-Capacity Endotoxin Removal Spin Columns (88274; ThermoFisher Scientific). Aliquots were stored at  $-20^{\circ}\text{C}$  for subsequent experiments.

**Stable transfection Chinese hamster ovary cells.** Chinese hamster ovary (CHO)–K1 (ATCC, CCL-61) cells were transfected with human ET<sub>A</sub>R (EDNRA, NM\_001957) Ohu22257C; GenScript Biotech) cloned into a pcDNA3.1<sup>+</sup>N-6His vector using PolyJet DNA Transfection Agent (SL100688; SignaGen) according to manufacturer's protocol. Briefly, 1  $\mu\text{g}$  of plasmid was added to cells (0.1 million cells/well) at low passage number in a 24-well plate. After seven days, cells were selected with geneticin (11811-064; Gibco) and single-cell sorted using a His-tag antibody (OAEA00010; Aviva). Functional expression of ET<sub>A</sub>R on clones was confirmed using ET-1 (HY-P0202; MedChemExpress).

**Cell culture.** Human telomerase reverse transcriptase (TERT)–immortalized human umbilical vein ECs (HUVECs/TERT2, CRL-4053, ATCC) were cultured on gelatin-coated dishes in vascular cell basal medium (ATCC-PCS-100-030, ATCC) supplemented with endothelial cell growth kit-VEGF (ATCC-PCS-100-041, ATCC), glutamax, 100 U/mL penicillin-streptomycin

(Pen-Strep), and 5% fetal calf serum (FCS). Medium was refreshed every two days, and cells were maintained at 37°C with 5% CO<sub>2</sub> until 80% to 90% confluence. CHO-K1 cells, CHO-ET<sub>A</sub>R, and commercially acquired CHO-AT<sub>1</sub> (ES-072-C; PerkinElmer) were cultured in Ham's F12 medium (21765029; Gibco) with 10% FCS and 100 U/mL of Pen-Strep. Additionally, for CHO-AT<sub>1</sub> and CHO-ET<sub>A</sub>R cells, 0.4 mg/mL of geneticin was added to maintain selection pressure. Cells were grown at 37°C under 5% CO<sub>2</sub> until 70% to 80% confluence.

**Stimulation of HUVEC for qPCR and ELISA.** HUVECs (p5–15) were seeded in gelatin-coated 12-well plates (0.1 million cells/well) and cultured overnight. Cells were serum-starved for one hour before pretreatment with 2 μM of valsartan (AT<sub>1</sub> antagonist, HY-18204; MedChemExpress) and 2 μM of BQ-123 (ET<sub>A</sub>R antagonist, HY-12378; MedChemExpress) or a vehicle (0.02% DMSO/phosphate buffered saline [PBS]) for one hour. Cells were then treated with 200 μg/mL of IgG, 10 μM of AngII (A9525; Sigma-Aldrich) with 10 μM of ET-1 (HY-P0202; MedChemExpress), 10 ng/mL of recombinant human tumor necrosis factor α (rhTNFα) (210-TA; R&D Systems), or medium. After 1 hour, a medium with FCS was added leading 1% FCS followed by incubation for 48 hours.

**RNA isolation and qPCR.** After 48 hours, HUVEC supernatant was collected, and cells were lysed in TRIzol (15596026; Invitrogen). RNA was isolated using the RNA Microprep Kit (R2063; Zymo Research) following the manufacturer's protocol. RNA concentration and purity were assessed using NanoDrop (Thermo Scientific). Next, 500 ng of RNA from each condition was mixed with the iScript complementary DNA (cDNA) Synthesis Kit (1708891; Bio-Rad) and supplemented to 20 μL with nuclease-free water (11538646; Invitrogen). qPCR was performed using 3 μL of diluted cDNA and 5 μL of master mix containing 2.5 pmol of forward and reverse primer, double distilled H<sub>2</sub>O, and SensiFAST SYBR No-ROX Kit (BIO-98005; Meridian Bioscience). Primer sequences are listed in Supplementary Table 2. The cDNA dilutions, primer concentrations, and standards were optimized according to the literature.<sup>30</sup> Mean cycle quantification (Cq) values were determined from technical replicates (n = 3). Relative quantity was calculated using  $(1+E)^{\Delta Cq}$ , in which *E* is the PCR efficiency from the standard curve, and Δ*Cq* is the difference between the sample and the medium control. Relative normalized expression was obtained by dividing the relative quantity of the target (intercellular adhesion molecule 1 [*ICAM1*], selectin E (*SELE*), C-C Motif Chemokine Ligand 2 [*CCL2*]) by the reference (beta-2-microglobulin [*B2M*]). Data were exported from CFX Maestro 3.2 (version 5.2; Bio-Rad) for statistical analysis.

**Cytokine ELISA.** Supernatants from IgG-stimulated HUVECs were analyzed for interleukin-6 (IL-6) (88-7066-88), IL-8 (88-8086-88), and TNFα (88-7346-88) using ELISA kits (Invitrogen) following the manufacturer's protocol. Briefly,

384-well plates (3700; Corning) were coated with 15 μL of antigen and blocked with 75 μL of 1% bovine serum albumin [BSA]/PBS. Diluted supernatant (IL-6, TNFα: 2×; IL-8: 10×), detection antibody, horseradish peroxidase (HRP)-labeled avidin antibody, and tetramethylbenzidine substrate (555214; BD Biosciences) were sequentially added (15 μL each). Reactions were stopped with 15 μL 1 M H<sub>2</sub>SO<sub>4</sub>, and absorbance was measured at 450 nm using a Multiskan Fc reader (Thermo Scientific). Cytokine standards (IL-6, IL-12: kit components; TNFα: 51-26376E; BD Biosciences) were used to calculate cytokine production when within the linear range.

**Real-time cell analysis.** Label-free, functional experiments were conducted using an xCELLigence RTCA (Agilent), which measures changes in impedance due to whole-cell responses, reflecting changes in cell number, proliferation rate, adhesion, and morphology expressed as the dimensionless parameter cell index (CI). This method is well-validated to study compound-receptor interactions.<sup>31–35</sup> All assays were performed at 37°C and 5% CO<sub>2</sub> in 96-well E-plates (300600900; Agilent) with 100 μL/well final volume. Background impedance was measured in 35 to 45 μL medium followed by the seeding of 40,000 cells/well. CI values were recorded every 15 minutes overnight. Cells were pretreated for one hour with 1 μM of an antagonist, 100 μg/mL of IgG, or a vehicle. Next, responses to 100 μM ATP, agonist, 200 μg/mL IgG or PBS were measured for 30 to 120 minutes. Compounds and IgG were added simultaneously to the E-plate using a VIAFLO 96-channel Handheld Electronic pipette (INTEGRA Biosciences). Experimental data were acquired using RTCA Software (version 2.2.1; Agilent). CI values were normalized just before compound or IgG addition to obtain normalized CI (nCI) values. Baseline corrections were made by subtracting vehicle control nCI values from each data point. Absolute net area under the curve (AUC) was calculated for the initial 60 minutes after stimulation (30 minutes for IgG pretreatment on CHO-ET<sub>A</sub>R cells). Net AUC data were analyzed with nonlinear regression in GraphPad Prism (version 9.3.1).

**Protein capture assay.** A novel protein assay using solubilized AT<sub>1</sub> was established to measure AT<sub>1</sub>-binding autoantibodies in SSC plasma. Solubilized GPCRs were obtained as described previously.<sup>36</sup> Briefly, epitope-tagged human GPCR constructs (AT<sub>1</sub>, CXCR3 [C-X-C motif chemokine receptor 3], cholinergic receptor muscarinic 3 [CHRM3]) with an N-terminal FLAG tag (DYKDDDDK) and C-terminal 1D4 tag (TETSQVAPA) were encoded in a pcDNA3.1+ mammalian expression vector. HEK293 FreeStyle cells were cultured according to manufacturer's instructions. One day before transfection, HEK293FS cells were diluted to 0.5 million cells/mL. The following day, 100 mL of cell suspension was transfected with plasmid DNA encoding CXCR3, CHRM3, or AT<sub>1</sub> using OptiMEM (12559099; Gibco) and 293fectin transfection reagent (10553283; Gibco).

Help vectors (p33-SV40LT, pORF-hp21V.16, pORF-hp27V02) were added to stop cell cycle and boost protein production, resulting in a final DNA concentration of 1  $\mu\text{g}/\text{mL}$ . For mock-transfected cells, only help vectors were added. After 24 hours, cells were harvested and washed with cold PBS. For each transfection, 500  $\mu\text{L}$  of cells was stained with anti-FLAG M2-fluorescein isothiocyanate (FITC) mouse monoclonal antibody (mAb) (1:200, F4049; Sigma-Aldrich) followed by flow cytometry to validate successful transfection. Remaining cells were solubilized using n-dodecyl- $\beta$ -D-maltoside (DDM) detergent (850520; Avanti) to form micelles to maintain GPCR conformation. Cells were incubated in solubilization buffer (50 mM HEPES, 1 mM EDTA, 150 mM NaCl, and 5 mM  $\text{MgCl}_2$  [pH 7.4]) with 1% (weight/volume) DDM and complete protease inhibitor (11836170001; Roche) for two hours at 4°C with head-over-head rotation. Lysates were clarified by centrifugation at 22,000g for 20 minutes at 4°C. Clarified solubilized membrane proteins were snap frozen in liquid nitrogen and stored at -80°C. Total protein concentration was determined using Pierce BCA protein assay (23227; Thermo Scientific) according to the manufacturer's protocol.

Plasma samples from 14 HDs and 28 patients with SSc were selected. Nunc MaxiSorp 96-well plate (430341; Thermo Scientific) were coated with 1  $\mu\text{g}/\text{mL}$  of rhodopsin monoclonal antibody (1D4) (MA1-722; Invitrogen) to capture solubilized GPCRs via their 1D4 epitope tag. After blocking with 1% BSA/PBS, solubilized GPCRs in solubilization buffer (with 1% BSA) were incubated for 30 minutes while shaking. Fractions of mock-transfected cells were included as negative control. Diluted plasma samples (1:100), anti-CXCR3 antibody (0.4  $\mu\text{g}/\text{mL}$ , HPA045942; Atlas Antibodies), anti-CHRM3 antibody (0.4  $\mu\text{g}/\text{mL}$ , HPA048036; Atlas Antibodies) and anti-DYKDDDDK tag (D6W5B) (2  $\mu\text{g}/\text{mL}$ , 14793S; Cell Signaling) were diluted in same buffer as solubilized GPCRs and incubated for one hour followed by incubation with 1:1,000 anti-human IgG/HRP (P0214; DAKO) or 1:7,500 anti-rabbit Ig/HRP (P0448; DAKO). Following extensive washing, plates were incubated with  $\text{H}_2\text{O}_2$ /ABTS. Absorbance at 415 nm was measured every 30 minutes.

**Statistical analysis.** Statistical analysis was performed with GraphPad Prism software (version 9.3.1). Variables are expressed as means  $\pm$  SEMs of three individually performed experiments with technical duplicates, unless otherwise specified. Statistical analysis was performed using Kruskal-Wallis test with Dunn's correction for nonparametric values, unless otherwise specified.  $P < 0.05$  was considered as statistically significant.

## RESULTS

### No EC activation upon stimulation with SSc IgG.

Because previous studies described a potential role for autoantibodies targeting  $\text{AT}_1$  and  $\text{ET}_A\text{R}$  resulting in EC

activation,<sup>13,18,37,38</sup> we set out to study the effect of SSc antibodies on endothelium by stimulation of human ECs with HD-derived IgG (HD IgG) and SSc IgG. Immortalized HUVECs were used to eliminate HUVEC donor-specific effects. First, as positive control, HUVECs were stimulated with 10 ng/mL of  $\text{TNF}\alpha$  for 48 hours to evaluate the up-regulation of *SELE*, *ICAM1*, and *CCL2*, all genes associated with EC activation. A fold change of 43.8 for *SELE*, 25.6 for *ICAM1*, and 13.1 for *CCL2* following  $\text{TNF}\alpha$  stimulation indicated the suitability of HUVEC as a model to study EC activation (Supplementary Figure 1). Next, isolated IgG from plasma samples from patients and HDs were used to minimize the potential influence of plasma components on vasculature, given the elevated levels of AngII and ET-1 in patients with SSc.<sup>11,12</sup> Although the addition of IgG fractions to HUVECs did induce a slight up-regulation of *SELE*, *ICAM1*, and *CCL2*, no differences were observed for SSc IgG ( $n = 5-10$ ) compared to HD IgG ( $n = 3$ ) (Figure 1A). Furthermore, stimulation with agonists AngII and ET-1 did not lead to EC activation. Likewise, pretreatment with  $\text{AT}_1$ -specific antagonist valsartan and  $\text{ET}_A\text{R}$ -specific antagonist BQ-123 did not attenuate the up-regulation of these markers.

Next, cytokine production by EC after stimulation with SSc and HD IgG was assessed. Although  $\text{TNF}\alpha$  stimulation of EC as positive control led to high cytokine production with optical density values outside the linear range (data not shown), no significant up-regulation of the proinflammatory cytokines IL-6, IL-8, or  $\text{TNF}\alpha$  was observed on stimulation with SSc IgG (Figure 1B). Altogether, these data suggest limited contribution of SSc IgG in EC activation.

Because the up-regulation of activation markers and proinflammatory cytokine production has been reported as a consequence of SSc IgG-induced  $\text{AT}_1$ - and/or  $\text{ET}_A\text{R}$ -mediated EC activation, we next aimed to study the potential direct effects of SSc IgG using another read-out. To this end, we took advantage of RTCA, a method to study cell morphologic effects of GPCR activation and previously applied to study EC responses.<sup>39</sup> HUVECs were stimulated with 100  $\mu\text{M}$  of ATP to define their non- $\text{AT}_1$ - or  $\text{ET}_A\text{R}$ -specific response window (Figure 1C), resulting in an average net AUC of 18.6. To study receptor-specific activation, HUVECs, either pretreated with specific antagonists or a vehicle, were stimulated with 10  $\mu\text{M}$  of AngII, 10  $\mu\text{M}$  of ET-1, or both. No effect of agonist stimulation was observed, both with and without antagonist pretreatment (Figure 1D). These results confirm our findings in Figure 1B showing limited effect of AngII with ET-1 stimulation on EC. To exclude differences in signaling between agonists and IgG, isolated IgG of HDs ( $n = 3$ ) and patients with SSc ( $n = 5$ ) was tested using RTCA. Similar to agonist stimulation, no activation of EC was observed on incubation with IgG (Figure 1E). Quantification of responses induced by HD IgG ( $n = 3$ ) and SSc IgG ( $n = 5$ ) showed no EC activation in an  $\text{AT}_1$ - or  $\text{ET}_A\text{R}$ -dependent manner (Figure 1F). In summary, stimulation of EC with SSc IgG did not provide evidence for EC activation in an  $\text{AT}_1$ - or  $\text{ET}_A\text{R}$ -dependent manner.

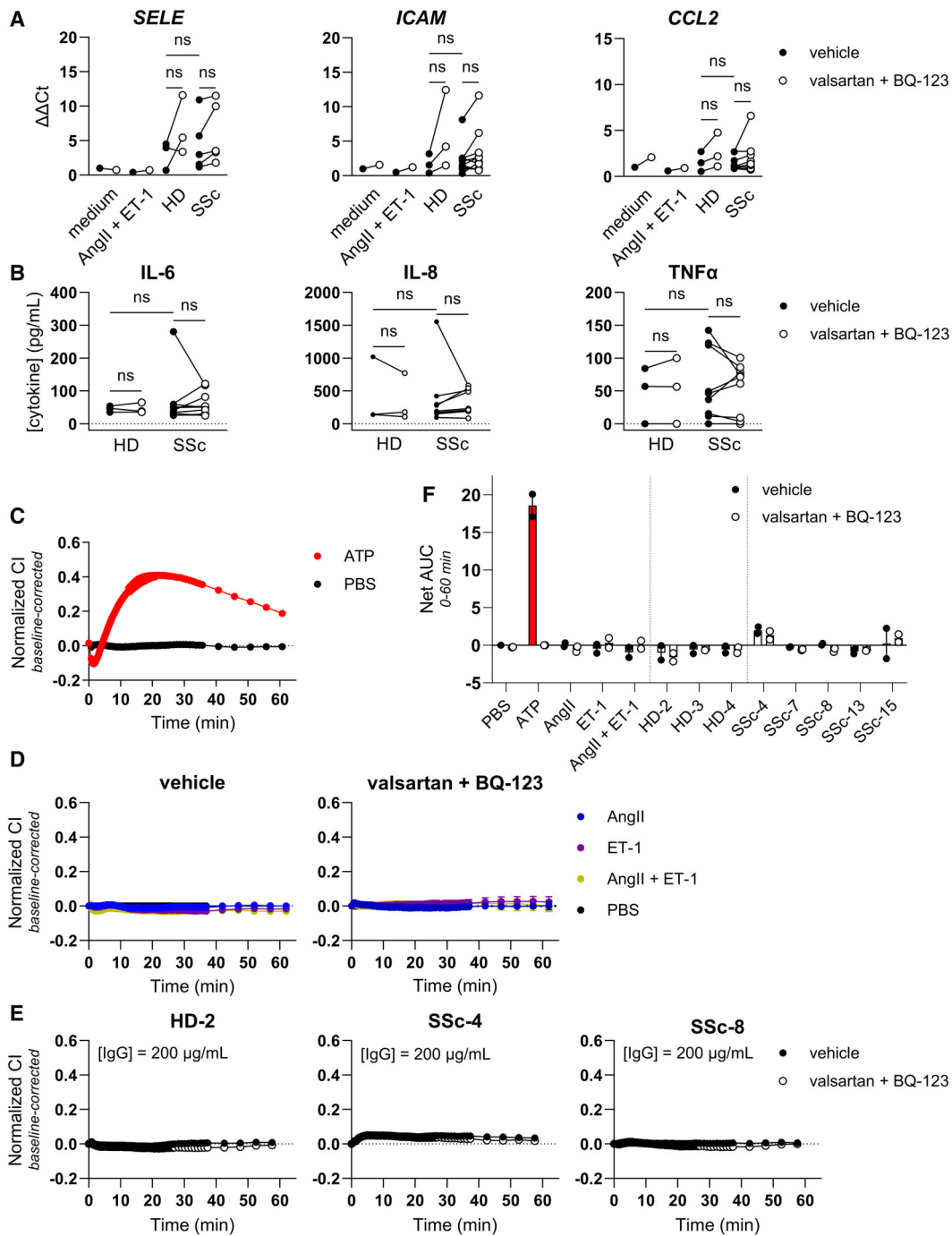


**Figure 1.** SSc IgG does not activate HUVECs in an AT<sub>1</sub>- or ET<sub>A</sub>R-mediated manner. (A)  $\Delta\Delta C_t$  of *SELE*, *ICAM1*, and *CCL2* in HUVECs pretreated with vehicle or 1  $\mu M$  of AT<sub>1</sub> antagonist valsartan plus ET<sub>A</sub>R antagonist BQ-123 followed by stimulation with 10  $\mu M$  of AngII plus ET-1 or 200  $\mu g/mL$  of IgG. Data points represent mean  $\Delta\Delta C_t$  measured in technical triplicates. (B) Cytokine ELISA for IL-6, IL-8, and TNF $\alpha$  with supernatant of HUVECs stimulated with 200  $\mu g/mL$  of IgG for 48 hours. Data points represent mean cytokine concentration measured in technical triplicates. (C) Representative graph of baseline-corrected real-time nCI traces of HUVECs stimulated with 100  $\mu M$  of ATP. (D) Representative graphs of baseline-corrected nCI traces of HUVECs pretreated with a vehicle or 1  $\mu M$  of valsartan plus BQ-123 before stimulation with 10  $\mu M$  of AngII, 10  $\mu M$  of ET-1, or both agonists. (E) Representative graphs of baseline-corrected nCI traces of HUVECs pretreated with a vehicle or 1  $\mu M$  antagonist before stimulation with 200  $\mu g/mL$  of IgG. (F) Net AUC (mean  $\pm$  SEM, n = 2) of HUVECs 0- to 60-minute baseline-corrected nCI traces pretreated with a vehicle or antagonist before stimulation with 10  $\mu M$  agonists or 200  $\mu g/mL$  of IgG. AngII, angiotensin II; AT<sub>1</sub>, angiotensin II receptor type 1; AUC, area under the curve; CI, cell index;  $\Delta\Delta C_t$ , gene expression fold change; *CCL2*, CC chemokine ligand 2; ET-1, endothelin-1; ET<sub>A</sub>R, endothelin-1 type A receptor; HD, healthy donor; HUVEC, human umbilical vein endothelial cell; *ICAM1*, intercellular adhesion molecule 1; IL-6, interleukin-6; nCI, normalized cell index; ns, not specific; PBS, phosphate buffered saline; *SELE*, selectin E; SSc, systemic sclerosis; TNF $\alpha$ , tumor necrosis factor  $\alpha$ . Color figure can be viewed in the online issue, which is available at <http://onlinelibrary.wiley.com/doi/10.1002/art.43099/abstract>.

**SSc IgG and the activation of AT<sub>1</sub> using an AT<sub>1</sub>-overexpressing CHO model.** Next, model cell lines overexpressing either human AT<sub>1</sub> (CHO-AT<sub>1</sub>) and human ET<sub>A</sub>R (CHO-ET<sub>A</sub>R) were established. These cell lines were characterized using RTCA to ensure potent and specific AngII- and ET-1-mediated activation of AT<sub>1</sub> and ET<sub>A</sub>R, respectively (Supplementary Figures 2 and 3).

Specificity of AngII for AT<sub>1</sub> was tested by stimulating parental (ie, nontransfected) CHO and CHO-AT<sub>1</sub> cells with 1 nM AngII (Figure 2A). No response was detected in the parental cells following AngII stimulation, whereas CHO-AT<sub>1</sub> exhibited an increasing response within the initial five minutes, indicating a potent and

functional AT<sub>1</sub> response. Pretreatment with 1  $\mu$ M AT<sub>1</sub> antagonist valsartan decreased net AUC by 74% compared to the response of vehicle-pretreated cells (Figure 2B), indicating the suitability of this model for studying selective AT<sub>1</sub> activation. Next, CHO-AT<sub>1</sub> cells were stimulated for 60 minutes with 200  $\mu$ g/mL of purified IgG of 4 HDs and 18 patients with SSc. As presented in Figure 2C, baseline-corrected nCI values did not reveal any response to IgG. Additionally, no discernible differences between HD and SSc IgG or in curve traces between cells pretreated with valsartan and those pretreated with vehicle could be observed. Quantification of responses into Net AUC showed no stimulatory effect of IgG, whereas stimulation with 1 nM AngII led to a potent

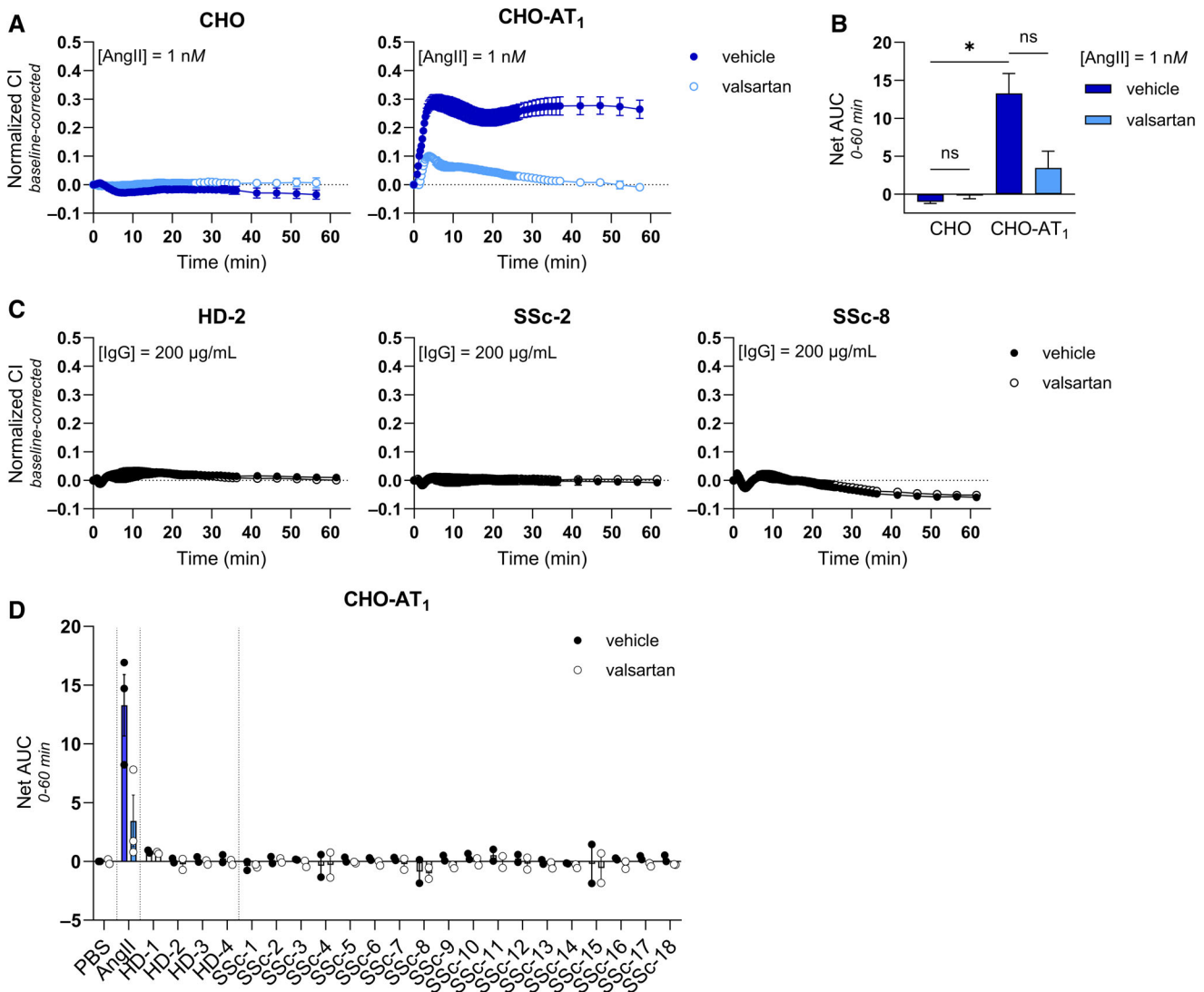


**Figure 2.** No observed effect of SSc IgG on CHO-AT<sub>1</sub> cells in an AT<sub>1</sub>-mediated manner. (A) Representative graphs of baseline-corrected nCI traces of CHO and CHO-AT<sub>1</sub> cells pretreated with vehicle or 1  $\mu$ M valsartan before stimulation with 1 nM AngII. (B) Net AUC (mean  $\pm$  SEM,  $n = 2-3$ ) of CHO and CHO-AT<sub>1</sub> 0- to 60-minute baseline-corrected nCI traces to 1 nM AngII. (C) Representative graphs of baseline-corrected nCI traces of CHO-AT<sub>1</sub> cells pretreated with vehicle or 1  $\mu$ M valsartan before stimulation with 200  $\mu$ g/mL of HD IgG or SSc IgG. (D) Net AUC (mean  $\pm$  SEM,  $n = 2-3$ ) of CHO-AT<sub>1</sub> 0- to 60-minute baseline-corrected nCI traces to 1 nM of AngII or 200  $\mu$ g/mL of IgG in absence and presence of 1  $\mu$ M valsartan on the individual level. AngII, angiotensin II; AT<sub>1</sub>, angiotensin II receptor type 1; AUC, area under the curve; CHO, Chinese hamster ovary; CI, cell index; HD, healthy donor; nCI, normalized cell index; ns, not specific; PBS, phosphate buffered saline; SSc, systemic sclerosis. Color figure can be viewed in the online issue, which is available at <http://onlinelibrary.wiley.com/doi/10.1002/art.43099/abstract>.

AT<sub>1</sub>-mediated response (Figure 2D). Taken together, we did not obtain evidence for AT<sub>1</sub>-mediated activation by SSc IgG in the highly sensitive CHO-AT<sub>1</sub> cells.

**SSc IgG and the activation of ET<sub>A</sub>R using an ET<sub>A</sub>R-overexpressing CHO model.** Similarly, the specificity of the endogenous ligand ET-1 for ET<sub>A</sub>R was confirmed by stimulating CHO and CHO-ET<sub>A</sub>R with 10 nM of ET-1 (Figure 3A). No response was observed in parental CHO cells on ET-1 stimulation, whereas CHO-ET<sub>A</sub>R displayed an increasing response in the first five minutes indicating functional expression of ET<sub>A</sub>R

in transfected cells. Pretreatment with specific ET<sub>A</sub>R antagonist BQ-123 decreased Net AUC by approximately 65% compared to the response of vehicle-pretreated cells (Figure 3B). Subsequently, isolated IgG from the same 4 HDs and 18 patients with SSc was used to stimulate CHO-ET<sub>A</sub>R cells. Analogous to the curve traces obtained with HUVEC and CHO-AT<sub>1</sub>R, no stimulatory effect of IgG on CHO-ET<sub>A</sub>R cells was revealed (Figure 3C). Additionally, no observable differences between HD and SSc IgG or in curve traces between cells pretreated with valsartan and those pretreated with a vehicle could be observed. Quantification of responses into net AUC showed no stimulatory effect

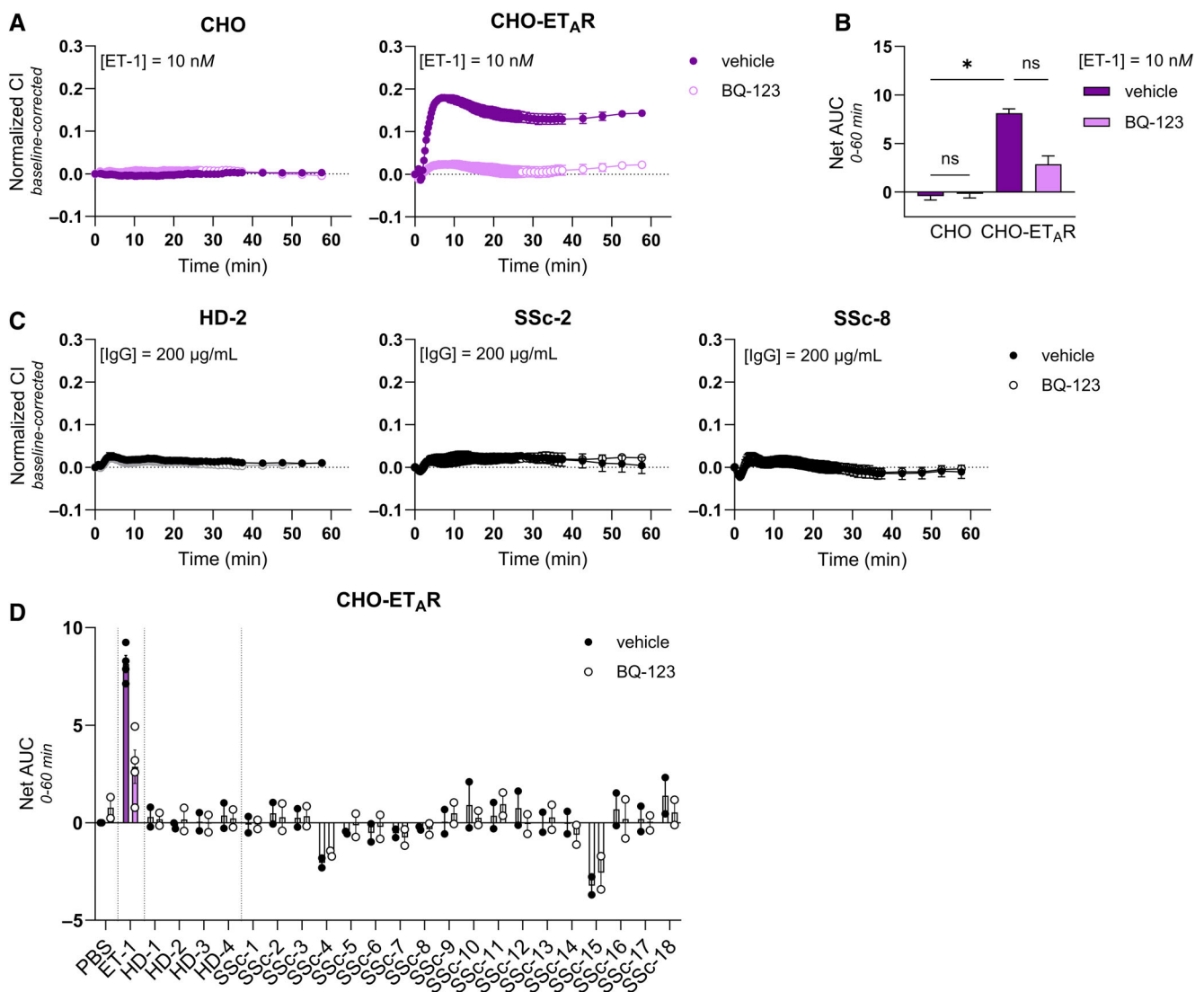


**Figure 3.** No observed effect of SSc IgG on CHO-ET<sub>A</sub>R cells in an ET<sub>A</sub>R-mediated manner. (A) Representative graphs of baseline-corrected nCI traces of CHO and CHO-ET<sub>A</sub>R cells pretreated with a vehicle or 1 μM of BQ-123 before stimulation with 10 nM of ET-1. (B) Net AUC (mean ± SEM, n = 2–4) of CHO and CHO-ET<sub>A</sub>R 0- to 60-minute baseline-corrected nCI traces to 10 nM ET-1. (C) Representative graphs of baseline-corrected nCI traces of CHO-ET<sub>A</sub>R cells pretreated with a vehicle or 1 μM BQ-123 before stimulation with 200 μg/mL of HD IgG or SSc IgG. (D) Net AUC (mean ± SEM, n = 2–4) of CHO-ET<sub>A</sub>R 0- to 60-minute baseline-corrected nCI traces to 10 nM ET-1 or 200 μg/mL of IgG in the absence and presence of 1 μM BQ-123 on an individual level. AUC, area under the curve; CHO, Chinese hamster ovary; CI, cell index; ET-1, endothelin-1; ET<sub>A</sub>R, endothelin-1 type A receptor; HD, healthy donor; nCI, normalized cell index; ns, not specific; PBS, phosphate buffered saline; SSc, systemic sclerosis. Color figure can be viewed in the online issue, which is available at <http://onlinelibrary.wiley.com/doi/10.1002/art.43099/abstract>.

of IgG whereas stimulation with 10 nM ET-1 led to an  $ET_A$ R-mediated response (Figure 3D). Overall, similar to results obtained in CHO-AT<sub>1</sub> cells, there was no observed evidence for  $ET_A$ R activation by SSc IgG on CHO- $ET_A$ R cells.

**No evidence for allosteric effect of SSc IgG on AngII response in CHO-AT<sub>1</sub> model.** To test for allosteric modulation by SSc IgG, CHO-AT<sub>1</sub> cells were stimulated with AngII ( $10^{-9.5}$ ,  $10^{-8.5}$ , and  $10^{-7.5}$  M) to obtain response curves without any IgG pretreatment (Figure 4A). Selected AngII concentrations are within the linear range of the concentration-response curve (Supplementary Figure 2) to ensure detectability of changes in agonistic response. Next, CHO-AT<sub>1</sub> cells were pretreated with 100  $\mu$ g/mL of HD or SSc IgG followed by stimulation with AngII ( $10^{-9.5}$ ,  $10^{-8.5}$ , and  $10^{-7.5}$  M) for 60 minutes. No evident differences in curve traces were observed between cells without IgG pretreatment and those with IgG pretreatment (Figure 4B). Furthermore, IgG isolated from patients with SSc did not alter the response to AngII compared to cells pretreated with HD IgG. Quantification of the responses into the net AUC confirmed no significant difference in AngII response between HD and SSc IgG-pretreated cells (Figure 4C). Altogether, these data do not provide evidence for altered AT<sub>1</sub> signaling on AngII stimulation after pretreatment with SSc IgG.

**No evidence for allosteric effect of SSc IgG on ET-1 response in CHO- $ET_A$ R model.** Similarly, CHO- $ET_A$ R cells were stimulated with ET-1 ( $10^{-9}$ ,  $10^{-8}$ , and  $10^{-7}$  M) to obtain responses without any IgG pretreatment (Figure 5A). Next, cells were pretreated with 100  $\mu$ g/mL of HD or SSc IgG pretreatment followed by ET-1 ( $10^{-9}$ ,  $10^{-8}$ , and  $10^{-7}$  M) stimulation for 30 minutes. IgG-pretreated cells showed no observable differences in curve traces compared to vehicle-pretreated cells (Figure 5B). Additionally, SSc IgG pretreatment did not affect the response to ET-1 compared to pretreatment with HD IgG. Quantification of the responses into the net AUC confirmed no significant difference in net AUC between HD and SSc IgG-pretreated cells (Figure 5C). Altogether, these data do not provide evidence for altered  $ET_A$ R signaling on ET-1 stimulation after pretreatment with SSc IgG.

**No AT<sub>1</sub>-binding IgG detected in SSc plasma using solubilized membrane proteins.** Given the absence of direct functional or response-modifying effects of SSc IgG in an AT<sub>1</sub>- or  $ET_A$ R-dependent manner, a new protein capture assay independent of receptor activation was established to detect the potential presence GPCR-binding autoantibodies. In this assay, the GPCRs retain their 3D-conformational integrity in detergent micelles. Epitope-tagged AT<sub>1</sub> was expressed and solubilized into

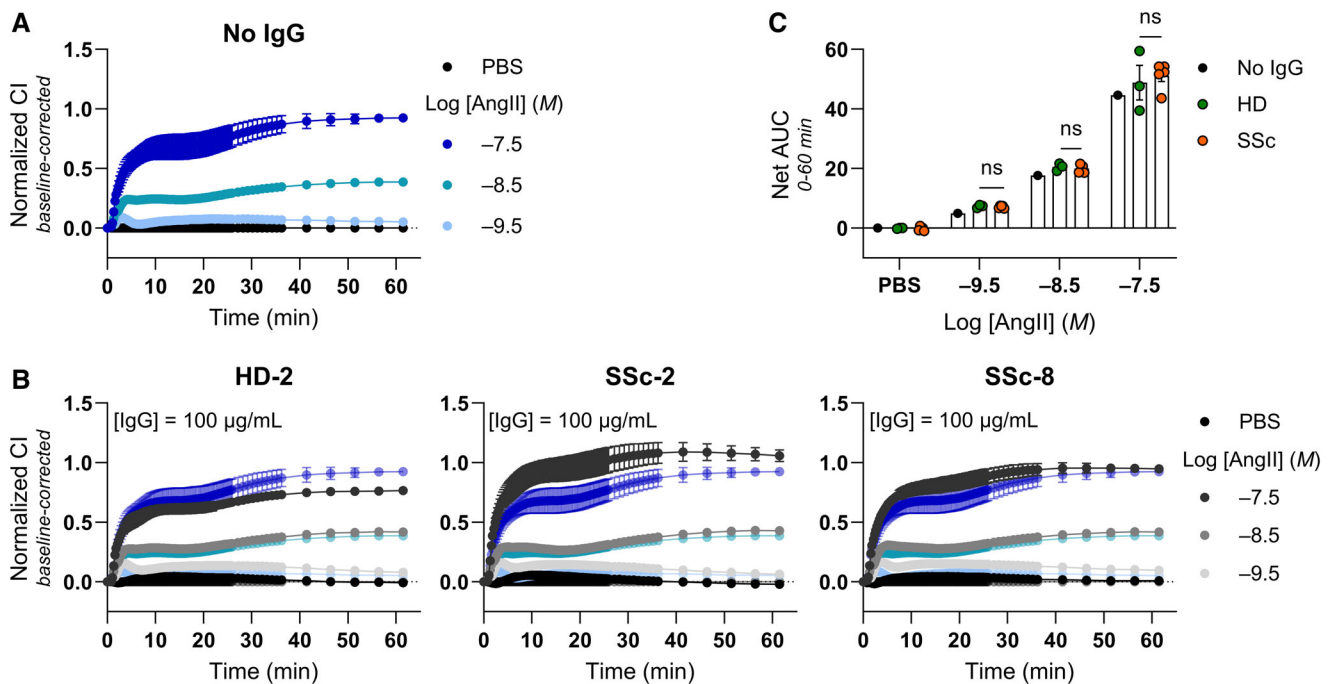


**Figure 4.** Pretreatment with SSc IgG does not alter AngII responses in CHO-AT<sub>1</sub> cells. (A) Representative graph of baseline-corrected normalized CI traces of CHO-AT<sub>1</sub> cells stimulated with  $10^{-9.5}$  to  $10^{-7.5}$  M AngII without any IgG pretreatment. (B) Representative graphs of CHO-AT<sub>1</sub> cells pretreated with 100  $\mu$ g/mL of HD IgG or IgG derived from patients with SSc before stimulation with  $10^{-9.5}$  to  $10^{-7.5}$  M AngII. (C) Net AUC (mean  $\pm$  SEM) of CHO-AT<sub>1</sub> cells pretreated with 100  $\mu$ g/mL of IgG before stimulation with AngII. Dots represent mean net AUC of two individual performed experiments with technical duplicates. Statistical analysis using the Mann-Whitney U-test with Dunn's correction for multiple testing. AngII, angiotensin II; AT<sub>1</sub>, angiotensin II receptor type 1; AUC, area under the curve; CHO, Chinese hamster ovary; CI, cell index; HD, healthy donor; ns, not significant; PBS, phosphate buffered saline; SSc, systemic sclerosis.

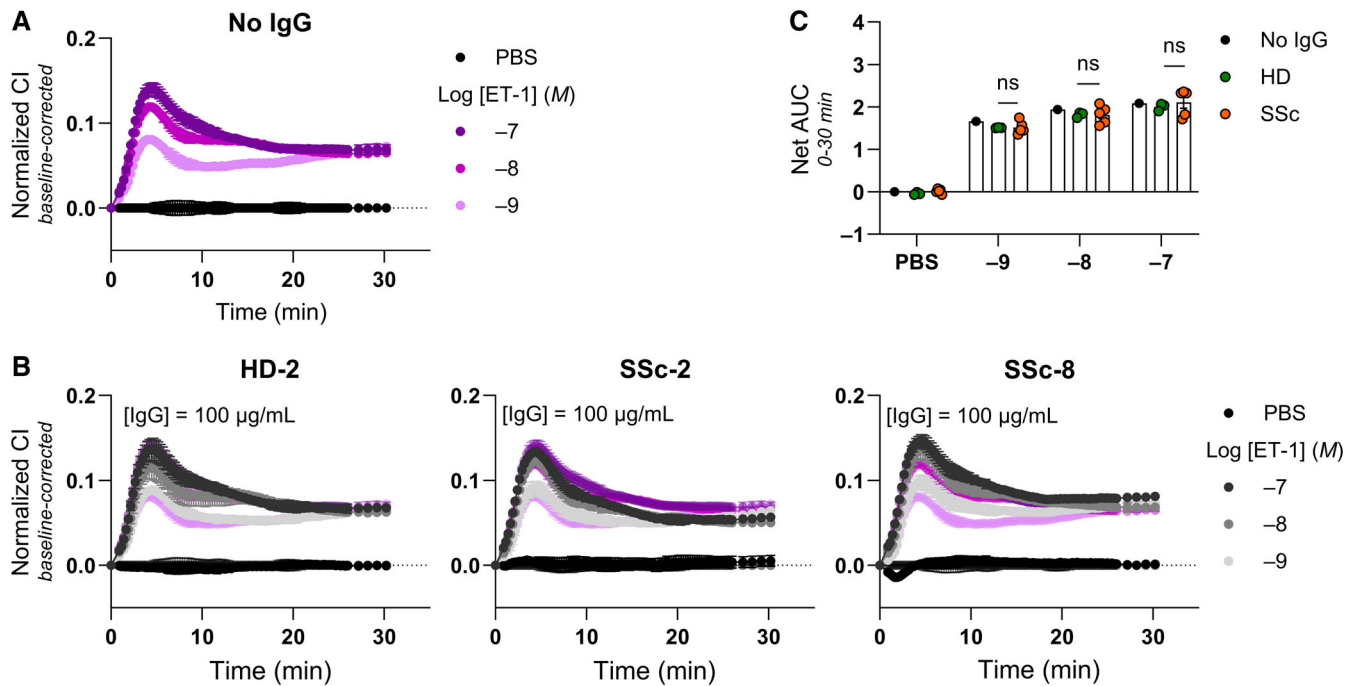


**Figure 5.** Pretreatment with SSc IgG does not alter ET-1 responses in CHO-ET<sub>A</sub>R cells. (A) Representative graph of baseline-corrected normalized CI traces of CHO-ET<sub>A</sub>R cells stimulated with 10<sup>-9</sup> to 10<sup>-7</sup> M ET-1 without any IgG pretreatment. (B) Representative graphs of CHO-ET<sub>A</sub>R cells pretreated with 100 µg/mL of HD IgG or SSc IgG before stimulation with 10<sup>-9</sup> to 10<sup>-7</sup> M ET-1. (C) Net AUC (mean ± SEM) of CHO-ET<sub>A</sub>R cells pretreated with 100 µg/mL of IgG before stimulation with ET-1. Dots represent mean net AUC of two individual performed experiments with technical duplicates. Statistical analysis using the Mann-Whitney U-test with Dunn’s correction for multiple testing. AUC, area under the curve; CHO, Chinese hamster ovary; CI, cell index; ET-1, endothelin-1; ET<sub>A</sub>R, endothelin-1 type A receptor; HD, healthy donor; ns, not significant; PBS, phosphate buffered saline; SSc, systemic sclerosis.

micelles as described in the material and methods section. Before solubilization, the presence of AT<sub>1</sub> in transfected cells was confirmed via the N-terminal FLAG tag using flow cytometry (Supplementary Figure 4). Solubilized GPCRs were added to anti-1D4-coated wells to capture GPCRs via their C-terminal

1D4 tag (Figure 6A). Solubilized membrane fractions from non-transfected cells (MOCK) were used as negative controls. None of the antibodies exhibited reactivity toward MOCK, whereas anti-CXCR3 and anti-CHRM3 antibodies displayed binding only to their respective solubilized GPCRs, confirming the specificity

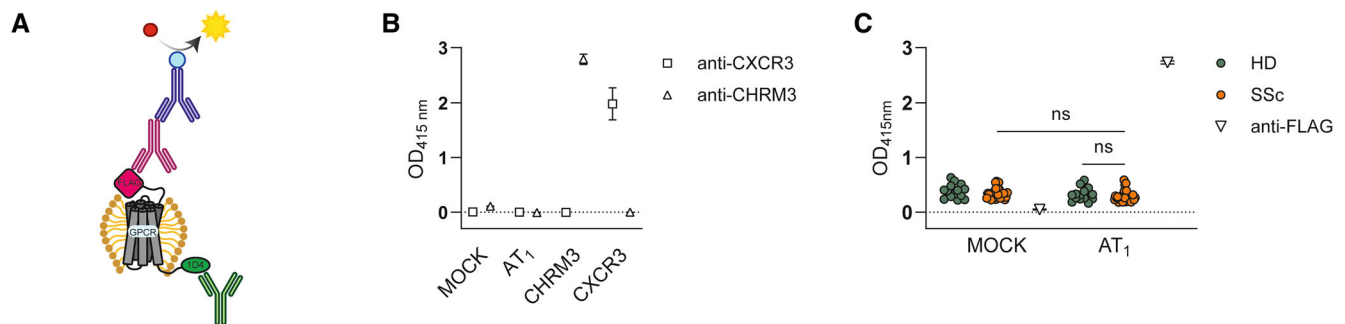


**Figure 6.** Detection of AT<sub>1</sub>-binding IgG in circulation using protein capture assay. (A) Schematic figure of the protein capture assay using wells coated with 1 µg/mL of anti-1D4 tag antibody to capture solubilized GPCRs followed by detection with anti-FLAG tag antibody as positive control. (B) OD<sub>415 nm</sub> values (mean ± SEM) of 0.4 µg/mL of anti-CXCR3 and 0.4 µg/mL of anti-CHRM3 antibodies toward 100 µg/mL of solubilized AT<sub>1</sub>, CHRM3, and CXCR3. MOCK as negative control. (C) OD<sub>415 nm</sub> values (mean ± SEM) of 1:100 diluted plasma samples towards 100 µg/mL solubilized membrane proteins of MOCK- or AT<sub>1</sub>-transfected HEK293-FreeStyle cells. 2 µg/mL of anti-FLAG tag antibody was included as positive control. Dots represent average OD value of SSc plasma (n = 28) or HD plasma (n = 14) measured in duplicate. AT<sub>1</sub>, angiotensin II receptor type 1; CHRM3, cholinergic receptor muscarinic 3; CXCR3, CXC Motif Chemokine Receptor 3; GPCR, G protein-coupled receptor; HD, healthy donor; MOCK, nontransfected cells; SSc, systemic sclerosis.

and sensitivity of this assay as well as the feasibility detection of the GPCRs (Figure 6B). Next, plasma samples from 28 patients with SSc, along with plasma samples of 14 HDs, were analyzed for AT<sub>1</sub>-binding IgG using HRP-labeled anti-human IgG. Compared to MOCK, OD values for solubilized AT<sub>1</sub> did not increase for both HD and SSc plasma, whereas for anti-FLAG OD values increased from 0.05 to 2.7 (Figure 6C). Furthermore, no differences in AT<sub>1</sub>-binding between HD and SSc plasma samples were detected. These findings do not provide evidence for the presence of AT<sub>1</sub>-binding autoantibodies in circulation of patients with SSc and are in line with the other performed experiments.

## DISCUSSION

SSc is a severe autoimmune disease marked by dysregulated immunity, fibrosis, and vasculopathy, with no existing cure. Given the early occurrence of vasculopathy in disease pathogenesis, it is essential for early intervention to understand the factors contributing to EC dysregulation and exaggerated vasoconstriction. Previous studies have described autoantibodies targeting AT<sub>1</sub> and ET<sub>A</sub>R, two receptors pivotal to blood pressure homeostasis, as relevant contributors to the pathogenesis of SSc. These autoantibodies are described to activate their respective receptors, which leads to abnormal vasoconstriction and subsequent microangiopathy, implying potential involvement of anti-AT<sub>1</sub>- and anti-ET<sub>A</sub>R autoantibodies in SSc pathogenesis.<sup>16,37</sup> However, the functional effects of anti-AT<sub>1</sub>- and anti-ET<sub>A</sub>R autoantibodies have primarily been explored through nonspecific markers situated downstream in the GPCR signaling cascade, leaving their receptor-specific effects unclear.<sup>19,38</sup> In this study, we employed a combination of conventional techniques such as qPCR and ELISA, alongside a robust platform measuring morphologic changes on GPCR activation to investigate the functional effects of SSc IgG. Additionally, we established a novel protein capture assay using solubilized AT<sub>1</sub> in micelles to screen for anti-AT<sub>1</sub>-binding autoantibodies in circulation. Despite using various techniques and different cell lines, our results do not provide evidence supporting the presence or functional role of AT<sub>1</sub>- or ET<sub>A</sub>R-binding autoantibodies in SSc IgG or the presence of AT<sub>1</sub>-binding autoantibodies in the circulation of patients with SSc.

The absence of a “positive” SSc-derived autoantibody-mediated signal could be a consequence of multiple factors. Our observations revealed no evidence of EC activation following incubation with SSc IgG, regardless of pretreatment with AT<sub>1</sub>- and ET<sub>A</sub>R-specific antagonists. Previous studies reported increased messenger RNA and protein levels of IL-8 and vascular cell adhesion molecule 1 after the incubation of ECs with SSc IgG in an AT<sub>1</sub>- and ET<sub>A</sub>R-dependent manner.<sup>18</sup> However, these effects displayed high levels of variability and varied between EC donors. Therefore, possible EC donor-specific effects and a contribution of autoantibodies other than anti-AT<sub>1</sub> and anti-ET<sub>A</sub>R to EC activation cannot be excluded, potentially

explaining differences in outcome. Another study reported EC proliferation and coagulation on stimulation with SSc IgG, resulting in extracellular signal-regulated kinase (ERK)1/2 phosphorylation in an AT<sub>1</sub>- and ET<sub>A</sub>R-dependent manner.<sup>38</sup> In the same study, stimulation with AngII and ET-1 did not show up-regulated ERK1/2 phosphorylation, which argues for AT<sub>1</sub>- and ET<sub>A</sub>R-independent effects. Similar findings were observed in another study,<sup>40</sup> in which no up-regulation of pERK1/2, mechanistic target of rapamycin complex 1 (mTORC1), or mTORC2 was detected following stimulation with AngII or ET-1. These findings align with our results, in which stimulation with AngII or ET-1 did not result in the up-regulation of markers for EC activation or a direct AT<sub>1</sub>- or ET<sub>A</sub>R-mediated response, as measured with RTCA. Overall, our data indicate no AT<sub>1</sub>- or ET<sub>A</sub>R-dependent activation of EC by SSc IgG, and neither could agonist-mediated activation of EC be detected. This raises questions regarding the suitability of EC to study the presence and effects of AT<sub>1</sub>- and ET<sub>A</sub>R-activating autoantibodies in total IgG derived from patients with SSc.

Considering the reported low endogenous expression levels of GPCRs on human cells,<sup>24,41–44</sup> it is possible that AT<sub>1</sub> and ET<sub>A</sub>R expression on HUVECs might be insufficient to detect activation of these receptors by SSc IgG. Therefore, we established models using CHO cells that overexpress the human AT<sub>1</sub> and ET<sub>A</sub>R, respectively to study these receptors. Agonist-mediated responses were measured in real-time, which could be effectively blocked with receptor-specific antagonists, confirming the suitability of this method to study AT<sub>1</sub> and ET<sub>A</sub>R activation specifically and sensitively. However, while activation of AT<sub>1</sub> and ET<sub>A</sub>R was observed upon stimulation with AngII and ET-1 respectively, no such effects were detected when using SSc IgG. Although some individuals displayed minimal changes in net AUC compared to control, the curve traces remained comparable irrespective of antagonist pretreatment. This suggests that any observed changes in impedance are likely not attributable to AT<sub>1</sub>- or ET<sub>A</sub>R activation.

Instead of direct activation, autoantibodies may alter the affinity of the natural agonist for the orthosteric binding pocket through allosteric modulation, a phenomenon previously described<sup>45</sup> for AT<sub>1</sub>. Allosteric ligands blocked the binding of rat polyclonal IgG to extracellular loop 2, thereby attenuating AngII-mediated signaling. While previous studies detected changes in intracellular Ca<sup>2+</sup> levels when incubating CHO cells transiently expressing AT<sub>1</sub> with precipitated SSc IgG before stimulation with AngII,<sup>46</sup> our study did not observe changes in net AUC values following the incubation of CHO-AT<sub>1</sub> or CHO-ET<sub>A</sub>R with SSc IgG compared to controls. Differences in outcome could potentially be explained by discrepancies in preparation methods of IgG fractions, the concentration of AngII used for stimulation, and the use of transiently transfected cells.

We developed a novel protein capture assay to screen for AT<sub>1</sub>-binding autoantibodies in SSc plasma to distinguish between

the functionality and binding characteristics of autoantibodies. To minimize interference of nuclear antigens, AT<sub>1</sub> was solubilized into micelles and captured via their 1D4-tag using antibody-coated wells. Micelles containing solubilized, epitope-tagged CXCR3 and CHRM3 were included as technical controls for GPCR conformation after solubilization, as well-validated antibodies are available for these two GPCRs, unlike AT<sub>1</sub> and ET<sub>A</sub>R.<sup>47</sup> Despite the presence of AT<sub>1</sub>, OD values of all plasma samples toward solubilized AT<sub>1</sub> were consistently low and comparable to values using solubilized membrane fractions of nontransfected cells, in which tag-specific capturing is not applicable. Furthermore, OD values of plasma samples from patients with SSc toward AT<sub>1</sub> did not differ from those of plasma from HDs. These observations argue against the presence of AT<sub>1</sub>-binding autoantibodies in the circulation of patients with SSc. It would, therefore, be of relevance to scrutinize whether the commercially available assays used for detecting anti-AT<sub>1</sub> and anti-ET<sub>A</sub>R reactivity could effectively detect antibodies against other antigens such as nuclear or cytoplasmic proteins. Unfortunately, protocols and reagents for these assays have not been shared, complicating such endeavors. Previous studies reported a strong correlation between ATA and anti-AT<sub>1</sub> and anti-ET<sub>A</sub>R autoantibodies. Additionally, high prevalence of positive reactivity was observed in plasma samples from other diseases associated with ANA, whereas samples from diseases with no known ANA levels were nearly negative.<sup>46</sup> Further research into the specificity of these commercial assays is needed to exclude the possibility of detected ANA instead of the presumed AT<sub>1</sub>- and ET<sub>A</sub>R-binding autoantibodies in plasma derived from patients with SSc.

Finally, while multiple reports described the presence of AT<sub>1</sub>- and ET<sub>A</sub>R-binding autoantibodies in association with clinical manifestations in SSc,<sup>16,19,38,40,48</sup> other reports found no correlation between the presence of these autoantibodies and clinical disease manifestations.<sup>2,49</sup> This discrepancy raises questions about the clinical relevance of these autoantibodies in to identify and discriminate patients with SSc, leaving their role in SSc pathogenesis is unclear. Similar observations have been described for autoantibodies targeting platelet-derived growth factor receptor (PDGFR). Initial reports suggested that stimulatory anti-PDGFR autoantibodies were a disease-specific hallmark of SSc.<sup>50</sup> Later studies detected these autoantibodies in the sera of HDs and without agonistic activity, highlighting the uncertain clinical significance and technical challenges in determining the role of functional autoantibodies in SSc pathogenesis.<sup>51,52</sup>

It is essential to acknowledge certain limitations in our study. Firstly, the sample size employed in functional studies, comprising 4 HDs and 18 patients with SSc, may be considered relatively small, particularly given the heterogeneous nature of SSc. Moreover, the use of cell lines to investigate AT<sub>1</sub> and ET<sub>A</sub>R activation by autoantibodies could be considered artificial compared to the natural physiologic environment. Another limitation of our study is the absence of an anti-AT<sub>1</sub> or anti-ET<sub>A</sub>R agonistic antibody,

which could have served as positive control to further validate the assays used in our study. Although in one study an anti-AT<sub>1</sub>-activating mAb was described, it was generated by immunizing mice with membrane extracts of human AT<sub>1</sub>-expressing CHO cells, making it disease unspecific.<sup>53</sup> Furthermore, its production relied on the screening of mouse hybridoma culture supernatants for anti-AT<sub>1</sub> antibodies using the commercially available anti-AT<sub>1</sub> ELISA, of which the specificity has been questioned in this article.<sup>53</sup> Although our study did not observe changes in AngII- or ET-1-mediated signaling on incubation with SSc IgG using RTCA, it is possible that long-lasting effects targeting different pathways been overlooked. However, the lack of responses observed in HUVECs over a 48-hour time interval on incubation with SSc IgG does not support a major role for long-lasting signaling pathways. Lastly, while we assessed presence of AT<sub>1</sub>-binding autoantibodies in circulation was assessed, there is currently no data available regarding ET<sub>A</sub>R-binding autoantibodies.

In summary, our study did not yield evidence supporting the presence of AT<sub>1</sub>- or ET<sub>A</sub>R-activating autoantibodies in purified SSc IgG. Both direct agonistic effect as well as modulated responses of the natural agonist were assessed. Furthermore, we did not detect AT<sub>1</sub>-binding IgG in circulation of patients with SSc. Because the correlation to disease manifestations and specificity to SSc pathogenesis remains controversial, the clinical relevance of using anti-AT<sub>1</sub> and anti-ET<sub>A</sub>R autoantibodies as biomarkers in SSc becomes unclear.

## ACKNOWLEDGMENTS

The authors thank Dr Riemekasten and her colleagues for measuring the anti-AT<sub>1</sub> and anti-ET<sub>A</sub>R antibody levels in serum with their solid phase ELISA, as published previously.<sup>19</sup>

## AUTHOR CONTRIBUTIONS

All authors contributed to at least one of the following manuscript preparation roles: conceptualization AND/OR methodology, software, investigation, formal analysis, data curation, visualization, and validation AND drafting or reviewing/editing the final draft. As corresponding author, Dr Fehres confirms that all authors have provided the final approval of the version to be published, and takes responsibility for the affirmations regarding article submission (eg, not under consideration by another journal), the integrity of the data presented, and the statements regarding compliance with institutional review board/Declaration of Helsinki requirements.

## REFERENCES

1. Denton CP, Khanna D. Systemic sclerosis. *Lancet* 2017;390(10103):1685–1699.
2. Lemmers JM, van Caam AP, Kersten B, et al. Nailfold capillaroscopy and candidate-biomarker levels in systemic sclerosis-associated pulmonary hypertension: a cross-sectional study. *J Scleroderma Relat Disord* 2023;8(3):221–230.
3. van Leeuwen NM, Liem SIE, Maurits MP, et al. Disease progression in systemic sclerosis. *Rheumatology (Oxford)* 2021;60(3):1565–1567.

4. Wortel CM, Liem SI, van Leeuwen NM, et al. Anti-topoisomerase, but not anti-centromere B cell responses in systemic sclerosis display active, Ig-secreting cells associated with lung fibrosis. *RMD Open* 2023;9(3):e003148.
5. Wigley FM. Clinical practice. Raynaud's phenomenon. *N Engl J Med* 2002;347(13):1001–1008.
6. Weir MR, Dzau VJ. The renin-angiotensin-aldosterone system: a specific target for hypertension management. *Am J Hypertens* 1999; 12(12 Pt 3):205S–213S.
7. Dziadzio M, Denton CP, Smith R, et al. Losartan therapy for Raynaud's phenomenon and scleroderma: clinical and biochemical findings in a fifteen-week, randomized, parallel-group, controlled trial. *Arthritis Rheum* 1999;42(12):2646–2655.
8. Böhm F, Pernow J. The importance of endothelin-1 for vascular dysfunction in cardiovascular disease. *Cardiovasc Res* 2007;76(1):8–18.
9. Steen VD, Costantino JP, Shapiro AP, et al. Outcome of renal crisis in systemic sclerosis: relation to availability of angiotensin converting enzyme (ACE) inhibitors. *Ann Intern Med* 1990;113(5):352–357.
10. Bütikofer L, Varisco PA, Distler O, et al; EUSTAR collaborators. ACE inhibitors in SSc patients display a risk factor for scleroderma renal crisis—a EUSTAR analysis. *Arthritis Res Ther* 2020;22(1):59.
11. Matucci-Cerinic M, Denton CP, Furst DE, et al. Bosentan treatment of digital ulcers related to systemic sclerosis: results from the RAPIDS-2 randomised, double-blind, placebo-controlled trial. *Ann Rheum Dis* 2011;70(1):32–38.
12. Kawaguchi Y, Takagi K, Hara M, et al. Angiotensin II in the lesional skin of systemic sclerosis patients contributes to tissue fibrosis via angiotensin II type 1 receptors. *Arthritis Rheum* 2004;50(1):216–226.
13. Seibold JR, Denton CP, Furst DE, et al. Randomized, prospective, placebo-controlled trial of bosentan in interstitial lung disease secondary to systemic sclerosis. *Arthritis Rheum* 2010;62(7):2101–2108.
14. Khanna D, Denton CP, Merkel PA, et al; DUAL-1 Investigators; DUAL-2 Investigators. Effect of macitentan on the development of new ischemic digital ulcers in patients with systemic sclerosis: Dual-1 and Dual-2 randomized clinical trials. *JAMA* 2016;315(18):1975–1988.
15. Galiè N, Barberà JA, Frost AE, et al; AMBITION Investigators. Initial use of ambrisentan plus tadalafil in pulmonary arterial hypertension. *N Engl J Med* 2015;373(9):834–844.
16. Becker MO, Kill A, Kutsche M, et al. Vascular receptor autoantibodies in pulmonary arterial hypertension associated with systemic sclerosis. *Am J Respir Crit Care Med* 2014;190(7):808–817.
17. Reinsmoen NL, Lai CH, Heidecke H, et al. Anti-angiotensin type 1 receptor antibodies associated with antibody mediated rejection in donor HLA antibody negative patients. *Transplantation* 2010;90(12):1473–1477.
18. Kill A, Tabeling C, Undeutsch R, et al. Autoantibodies to angiotensin and endothelin receptors in systemic sclerosis induce cellular and systemic events associated with disease pathogenesis. *Arthritis Res Ther* 2014;16(1):R29.
19. Riemekasten G, Philippe A, Näther M, et al. Involvement of functional autoantibodies against vascular receptors in systemic sclerosis. *Ann Rheum Dis* 2011;70(3):530–536.
20. Wallukat G, Homuth V, Fischer T, et al. Patients with preeclampsia develop agonistic autoantibodies against the angiotensin AT1 receptor. *J Clin Invest* 1999;103(7):945–952.
21. Dragun D, Müller DN, Bräsen JH, et al. Angiotensin II type 1-receptor activating antibodies in renal-allograft rejection. *N Engl J Med* 2005; 352(6):558–569.
22. Bian J, Lei J, Yin X, et al. Limited AT1 receptor internalization is a novel mechanism underlying sustained vasoconstriction induced by AT1 receptor autoantibody from preeclampsia. *J Am Heart Assoc* 2019; 8(6):e011179.
23. Pearl MH, Chen L, Eichaki R, et al. Endothelin type A receptor antibodies are associated with angiotensin II type 1 receptor antibodies, vascular inflammation, and decline in renal function in pediatric kidney transplantation. *Kidney Int Rep* 2020;5(11):1925–1936.
24. Rosenbaum DM, Rasmussen SGF, Kobilka BK. The structure and function of G-protein-coupled receptors. *Nature* 2009;459(7245): 356–363.
25. Yang D, Zhou Q, Labroska V, et al. G protein-coupled receptors: structure- and function-based drug discovery. *Signal Transduct Target Ther* 2021;6(1):7.
26. Speck D, Kleinau G, Szczepek M, et al. Angiotensin and endothelin receptor structures with implications for signaling regulation and pharmacological targeting. *Front Endocrinol (Lausanne)* 2022;13:880002.
27. Li Y, Li B, Chen W-D, et al. Role of G-protein coupled receptors in cardiovascular diseases. *Front Cardiovasc Med* 2023;10:1130312.
28. Higuchi S, Ohtsu H, Suzuki H, et al. Angiotensin II signal transduction through the AT1 receptor: novel insights into mechanisms and pathophysiology. *Clin Sci (Lond)* 2007;112(8):417–428.
29. van den Hoogen F, Khanna D, Fransen J, et al. Classification criteria for systemic sclerosis: an American College of Rheumatology/European League against Rheumatism collaborative initiative. *Arthritis Rheum* 2013;65(11):2737–2747.
30. Taylor SC, Nadeau K, Abbasi M, et al. The ultimate qPCR experiment: producing publication quality, reproducible data the first time. *Trends Biotechnol* 2019;37(7):761–774.
31. Doornbos MLJ, Heitman LH. Label-free impedance-based whole cell assay to study GPCR pharmacology. *Methods Cell Biol* 2019;149: 179–194.
32. Doornbos MLJ, Van der Linden I, Vereyken L, et al. Constitutive activity of the metabotropic glutamate receptor 2 explored with a whole-cell label-free biosensor. *Biochem Pharmacol* 2018;152:201–210.
33. Ke N, Nguyen K, Irelan J, et al. Multidimensional GPCR profiling and screening using impedance-based label-free and real-time assay. *Methods Mol Biol* 2015;1272:215–226.
34. Chen ANY, Malone DT, Pabreja K, et al. Detection and quantification of allosteric modulation of endogenous m4 muscarinic acetylcholine receptor using impedance-based label-free technology in a neuronal cell line. *J Biomol Screen* 2015;20(5):646–654.
35. Hillger JM, le Roy B, Wang Z, et al. Phenotypic screening of cannabinoid receptor 2 ligands shows different sensitivity to genotype. *Biochem Pharmacol* 2017;130:60–70.
36. Lorenzen E, Dodig-Crnković T, Kotliar IB, et al. Multiplexed analysis of the secretin-like GPCR-RAMP interactome. *Sci Adv* 2019;5(9): eaaw2778.
37. Berger M, Steen VD. Role of anti-receptor autoantibodies in pathophysiology of scleroderma. *Autoimmun Rev* 2017;16(10):1029–1035.
38. Catar R, Herse-Naether M, Zhu N, et al. Autoantibodies targeting AT<sub>1</sub>- and ET<sub>A</sub>-receptors link endothelial proliferation and coagulation via Ets-1 transcription factor. *Int J Mol Sci* 2021;23(1):244.
39. Mocking TAM, van Oostveen WM, van Veldhoven JPD, et al. Label-free detection of prostaglandin transporter (SLCO2A1) function and inhibition: insights by wound healing and TRACT assays. *Front Pharmacol* 2024;15:1372109.
40. Catar RA, Wischniewski O, Chen L, et al. Non-HLA antibodies targeting angiotensin II type 1 receptor and endothelin-1 type A receptors induce endothelial injury via β2-arrestin link to mTOR pathway. *Kidney Int* 2022;101(3):498–509.
41. Fredriksson R, Schiöth HB. The repertoire of G-protein-coupled receptors in fully sequenced genomes. *Mol Pharmacol* 2005;67(5): 1414–1425.
42. Regard JB, Sato IT, Coughlin SR. Anatomical profiling of G protein-coupled receptor expression. *Cell* 2008;135(3):561–571.

43. Okuno K, Torimoto K, Cicalese SM, et al. Angiotensin II type 1A receptor expressed in smooth muscle cells is required for hypertensive vascular remodeling in mice infused with angiotensin II. *Hypertension* 2023;80(3):668–677.
44. Davenport AP, Hyndman KA, Dhaun N, et al. Endothelin. *Pharmacol Rev* 2016;68(2):357–418.
45. Singh KD, Jara ZP, Harford T, et al. Novel allosteric ligands of the angiotensin receptor AT1R as autoantibody blockers. *Proc Natl Acad Sci USA* 2021;118(33):e2019126118.
46. Bankamp L, Preuß B, Pecher AC, et al. Functionally active antibodies to the angiotensin II type 1-receptor measured by a luminometric bioassay do not correlate with clinical manifestations in systemic sclerosis: a comparison with antibodies to vascular receptors and topoisomerase I detected by ELISA. *Front Immunol* 2021;12:786039.
47. Dahl L, Kotliar IB, Bendes A, et al. Multiplexed selectivity screening of anti-GPCR antibodies. *Sci Adv* 2023;9(18):eadf9297.
48. Günther J, Kill A, Becker MO, et al. Angiotensin receptor type 1 and endothelin receptor type A on immune cells mediate migration and the expression of IL-8 and CCL18 when stimulated by autoantibodies from systemic sclerosis patients. *Arthritis Res Ther* 2014;16(2):R65.
49. İlgen U, Yayla ME, Düzgün N. Anti-angiotensin II type 1 receptor autoantibodies (AT<sub>1</sub>R-AAs) in patients with systemic sclerosis: lack of association with disease manifestations. *Rheumatol Int* 2017;37(4):593–598.
50. Baroni SS, Santillo M, Bevilacqua F, et al. Stimulatory autoantibodies to the PDGF receptor in systemic sclerosis. *N Engl J Med* 2006;354(25):2667–2676.
51. Balada E, Simeón-Aznar CP, Ordi-Ros J, et al. Anti-PDGFR- $\alpha$  antibodies measured by non-bioactivity assays are not specific for systemic sclerosis. *Ann Rheum Dis* 2008;67(7):1027–1029.
52. Loizos N, Lariccia L, Weiner J, et al. Lack of detection of agonist activity by antibodies to platelet-derived growth factor receptor  $\alpha$  in a subset of normal and systemic sclerosis patient sera. *Arthritis Rheum* 2009;60(4):1145–1151.
53. Yue X, Yin J, Wang X, et al. Induced antibodies directed to the angiotensin receptor type 1 provoke skin and lung inflammation, dermal fibrosis and act species overarching. *Ann Rheum Dis* 2022;81(9):1281–1289.